Adsorption (2013) 19:373–379
DOI 10.1007/s10450-012-9460-9

Experimental and theoretical study of D_2/H_2 quantum sieving in a carbon molecular sieve

A. Gotzias · G. Charalambopoulou ·
A. Ampoumogli · I. Krkljus · M. Hirscher ·
Th. Steriotis

Received: 31 October 2012 / Accepted: 21 December 2012 / Published online: 9 January 2013

Abstract The present work aims at providing additional insight into the crucial effect of pore size and pressure on the adsorption of H_2 and D_2 in porous carbons by means of Grand Canonical Monte Carlo simulations in model slit micropores at 77 K. In order to address the quantum behavior of the molecules the Feynman–Hibbs corrected LJ interaction potential is used for fluid–solid and fluid–fluid interactions. Based on the GCMC isotherms for the two isotopes, D_2 selectivity over H_2 is deduced for pores with different sizes as a function of pressure. Furthermore, GCMC results are coupled with experimental high pressure H_2 and D_2 adsorption data at 77 K for a commercial carbon molecular sieve (Takeda 3A).

Keywords H_2 adsorption · GCMC simulations · Pore size distribution · Carbon molecular sieves · Quantum sieving

1 Introduction

Carbon Molecular Sieves (CMS) comprise a technologically important family of porous carbons (Inagaki 2000) mainly characterised by the presence of narrow slit-shaped micropores of molecular dimensions (effective diameter between 0.4 and 0.9 nm), that allow the separation of molecular species based on size, shape or chemical affinity differences. Another attractive option is the possibility to use CMS as quantum sieves for separating isotopic (e.g. $H_2/D_2/T_2$) mixtures, a typically complex and demanding process due to the similar size and chemical properties of the individual components (Cai et al. 2012). Quantum separation occurs upon the preferential adsorption and/or faster kinetics of the heavier isotopes under spatial confinement. The concept of quantum molecular sieving was first introduced by Beenaker et al. (1995) who described the adsorption of hydrogen isotopes in a cylindrical pore using a simple deep potential well model. It was proposed that if the pore size becomes comparable with the de Broglie wavelength of an isotope, molecular adsorption and transport is controlled by quantum effects, originating from the different mass of the isotope molecules. Such effects were later confirmed both experimentally and theoretically for various adsorbents containing pores in the subnanometer region (Kaneko et al. 2012; Wang et al. 1999; Tanaka et al. 2005, 2009; Hattori et al. 2006; Noguchi et al. 2010; Hankel et al. 2012; Kagita et al. 2012; Liu et al. 2012; Viscor et al. 2012). At low temperatures and under confinement the translational motion of species is quantized leading to larger effective diameters for the lighter isotopes. In this way, narrow sized pores at low temperatures can possibly be more accessible to the heavier deuterium than hydrogen.

Based on the above it is clear that an appropriate porous sieve must contain a large population of pores with size comparable to hydrogen molecular dimensions to enable the efficient separation of its isotopic mixtures. As such quantum sieving performance is greatly affected by the

---

A. Gotzias · G. Charalambopoulou · A. Ampoumogli ·
Th. Steriotis (✉)
National Center for Scientific Research “Demokritos”,
15310 Ag. Paraskevi Attikis, Athens, Greece
e-mail: tster@chem.demokritos.gr

I. Krkljus · M. Hirscher
Max Planck Institute for Intelligent Systems,
Heisenbergstrasse 3, 70569 Stuttgart, Germany

Present Address:
I. Krkljus
BASF SE, Chemicals Research & Engineering,
67056 Ludwigshafen, Germany

pore size distribution (PSD) of the adsorbent matrix, i.e. the distribution of pore volume (or surface area) with respect to pore size.

PSD represents the most common way to describe a nanoporous material. The advance of computational tools and models have led to the widespread use of density functional theory (DFT) and GCMC simulations in model pore systems for PSD calculations based on the analysis of standard isothermal gas (e.g. N_2, Ar) adsorption measurements at cryogenic temperatures (Gregg and Sing 1982). Such an exercise is inevitably based upon a series of rough, and quite often oversimplified, assumptions about the actual architecture (e.g. pore shape/connectivity) and chemical composition of the porous network (Dombrowski et al. 2000; Gauden et al. 2006). For instance the microstructure of activated carbon materials, although inherently complex and disordered, is usually contemplated as a system of independent, slit-like pores with homogeneous, graphitic walls. The pore size distribution function, *f*(*H*), of this system can be determined by inverting the adsorption integral equation (Dombrowski et al. 2000; Jagiello et al. 2006; Konstantakou et al. 2007)

$$N(P) = \int_{H_{\min}}^{H_{\min}} n(P,H)f(H)dH \qquad (1)$$

where $N(P)$ is the is the experimentally measured adsorbed amount at bulk gas pressure P, $n(P, H)$ is the average density of adsorbate at pressure P in a single model graphitic slit pore of physical pore width H, while H_{min} and H_{max} correspond to the smallest and largest pore widths considered.

A reliable PSD analysis in the particular case of CMS, having pores in the subnanometer scale, requires in addition to a realistic representation of the overall structure, the use of “probe” molecules with sufficiently small size. The largest fraction of the CMS pore network may not be accessible to N_2 or Ar, the most commonly used “probe” adsorbate molecules, especially at cryogenic temperatures (Nguyen and Bhatia 2012; Jagiello and Thommes 2004) while concurrent diffusional limitations often met in microporous systems can lead to significant underestimation of the adsorption isotherm (Rodriguez-Reinoso and Linares-Solano 1988). It has been suggested that accessibility and kinetic constraints can be overcome, by using e.g. CO_2 at 273 K and especially H_2 at 77 K, which might provide more information in the ultra-micropore range (<0.7 nm) (Jagiello and Thommes 2004; Jagiello et al. 2006). H_2 is considered ideal for this purpose due to its small size, but also because it is supercritical gas at 77 K ensuring fast equilibration kinetics (Konstantakou et al. 2007). Wang and Bhatia (2009) used the CO2 (273 K) derived PSD of Takeda 3A (a commercially available CMS) to estimate its HD/H_2 selectivity at 40 and 77 K, based on path integral Monte Carlo simulations, while Nguyen et al. (2009) interpreted D_2 adsorption data on the same carbon.

The present work combines experimental and simulation studies aiming to provide additional insight into the crucial effect of pore size on the adsorption of hydrogen in microporous carbons but also to show that hydrogen adsorption data are highly useful for the characterization of carbon molecular sieves. The adsorption of H_2 and D_2 is studied by means of Grand Canonical Monte Carlo (GCMC) simulations in model graphitic slit micropores at 77 K and pressures up to 20 bar, based on an approach that we recently reported (Gotzias and Steriotis 2012). Based on the GCMC isotherms for the two isotopes, D_2 selectivity over H_2 is deduced for pores with different sizes as a function of pressure. It should be stressed that although it may be considered thermodynamically inaccurate, for simplicity we define here “selectivity” as the ratio of amounts adsorbed normalized by the ratio of bulk fluid densities. In a next step, GCMC results are coupled with experimental high pressure H_2 and D_2 adsorption data at 77 K for a commercial carbon molecular sieve, i.e. Takeda 3A with a nominal pore size in the range 0.3–0.4 nm. In brief, the experimental H_2 adsorption data are combined with the model H_2 adsorption isotherms (for individual pores) to derive the PSD of Takeda 3A carbon, which is then used for the calculation of the D_2 sorption isotherm at 77 K and pressures up to 20 bar. The calculated results are in good agreement with experimental high pressure D_2 adsorption data on Takeda 3A.

2 Experimental

Takeda 3A carbon (denoted hereafter as T3A), produced by carbon deposition on a microporous substrate resulting from the carbonization of a coconut shell, was provided from Takeda Chemical Industries Ltd., Japan (commercial code name: SHIRASAGI MSC-3 K-Type 172) in the form of cylindrical pellets with approximate diameter 1.9 mm.

H_2 and D_2 adsorption isotherms were measured at 77 K up to 20 bar, using a PCTPro-2000 automatic volumetric system (SETARAM). In each case appropriate outgassing of the sample (heat treatment at 250 °C for at least 24 h under high vacuum) was performed prior to measurement. Volume calibrations were carried out with helium at room temperature in order to minimize helium sorption errors at 77 K.

3 Simulation details

In order to derive the PSD of a microporous carbon matrix according to Eq. 1, it is necessary to construct the $n(P, H)$ kernel congregating model adsorption isotherms in isolated single pores of given widths. In this context, a previously reported GCMC approach (Gotzias and Steriotis 2012) was adapted for the simulation of H_2 and D_2 adsorption in single graphite slit-like pores. The pore walls were represented by parallel graphene honeycomb lattices placed at a varying distance H (noted also as H_{ph}) between 0.575 and 2.0 nm, defining the respective physical pore width. Taking into account that hydrogen and deuterium molecules confined in very narrow spaces at low temperatures, cannot be treated as classical Lennard–Jones (LJ) particles due to quantum effects, the Feynman–Hibbs corrected LJ interaction potential (Sese 1995; Wang et al. 1997; Stan and Cole 1998; Pantatosaki et al. 2008) was used to describe all solid–fluid and fluid–fluid interactions, according to:

$$U_{FH} = U_{LJ}(r) + \frac{\hbar^2}{24\mu k_B T}\nabla^2(U_{LJ}(r)) \tag{2}$$

where U_{LJ} denotes the classical LJ potential, $\hbar$ is the Planck's constant divided by 2π, T is the temperature, μ is the reduced mass of the interacting species and r is the distance between them. It should be mentioned that although this approach is considered adequate at 77 K, for lower temperatures more elaborate approaches (such as path integral methods) are required.

The same LJ parameters were used for hydrogen and deuterium (Table 1), while for deriving reduced mass, μ, it was assumed that $m_{H2} = 2.0159$ g/mol, $m_{D2} = 2 \cdot m_{H2}$ and $m_C = 12$ g/mol (contrary to commonly used mean field models, the calculation of μ also included the mass of carbon atoms to account for the interaction between the isotope adsorbate and the explicitly defined carbon atoms).

Single-component adsorption isotherms of H_2 and D_2 in carbon slit pores at 77 K were simulated in the grand canonical ensemble. Each adsorption isotherm constitutes of $n = 30$ pressure steps in the range $[P_0, P_{\max}] = [1 \times 10^{-4}, 20]$ bar. In brief, the simulation box contained the slit pore, with periodic boundary conditions and minimum image convection in x and y directions (the pore width lies in the z direction). The volume, temperature and chemical potential were fixed, while in each Monte Carlo step a random displacement, creation or deletion of a single fluid molecule was attempted with equal probability. The grand canonical ensemble utilized an adequate number of configurations in order to deduce the average values for the total adsorption energy $\langle U \rangle$ and the number of encountered particles $\langle N \rangle$. The chemical potential of the ensemble was then related to pressure according to $\mu(i) = k_B T \ln\left(P(i)\lambda^3 / k_B T\right)$. Here λ is the thermal de Broglie wavelength of a fluid molecule of mass m e.g. $\lambda = \hbar/\sqrt{m k_B T}$.

In order to correlate experimental data with the computed densities, the latter have to be expressed as excess adsorption, i.e.:

$$\Gamma_{ex} = \Gamma_{ads} - \rho_{bulk} V_{free} \tag{3}$$

where Γ_{ads} is the total amount adsorbed computed directly by GCMC (expressed by the total volume of the system), ρ_{bulk} is the bulk H_2 or D_2 gas density (e.g. obtained from the NIST database), and V_{free} is the free volume, namely the total volume of the system V_{ph} minus the volume occupied by the solid sorbent. The free volume of the pore can be estimated by a simple "Hit and miss" Monte Carlo volume integration of the pore space as explained by Do and Do (2006). According to this scheme, a "success" hit is registered when a randomly inserted ghost hydrogen molecule in the system volume, obtains non-positive solid–fluid energy. After millions of successive iterations the ratio V_{free}/V_{ph} converges. In our case the above ratio denotes also the H_{free}/H_{ph} ratio. According to our calculations H_{free} and H_{ph} obtain the relation: $H_{free} = 0.99 \cdot H_{ph} - 0.55$. The chemical or accessible width of the slit pore is then defined as $w = H_{free} + \sigma$, where $\sigma = \sigma_{H_2} = \sigma_{D_2}$ from Table 1.

Table 1 Potential model parameters used in GCMC simulations

Adsorbate	Lennard–Jones parameters			Reference
	σ (nm)	ε/k (K)	m (g)	
D_2	0.2958	36.7	2.016	Levesque et al. (2002)
H_2			4.028	
C (graphene)	0.340	37.26	12	Steele (1973), Nguyen (2009)

4 Results and discussion

4.1 GCMC H_2 and D_2 adsorption isotherms

Figure 1 presents the excess isotherms of H_2 and D_2 adsorption (expressed as excess adsorption densities versus pressure) at 77 K as calculated for an indicative set of slit pores with size 0.316, 0.391, 0.614, 0.738 and 1.036 nm. In all cases the adsorbed D_2 amount is higher than H_2, in good agreement with several theoretical and experimental studies (Kumar and Bhatia 2005; Kumar et al. 2006; Zhao et al. 2006; Chen et al. 2008; Xu et al. 2009; Wang and Bhatia 2009; Nguyen et al. 2010; Garberoglio and Johnson 2010). Hydrogen access to the extremely confined environment of the 0.316 nm pore is strongly hindered, resulting to very low adsorption densities even in the high pressure range. The effective size of this pore is just 0.02 nm wider than

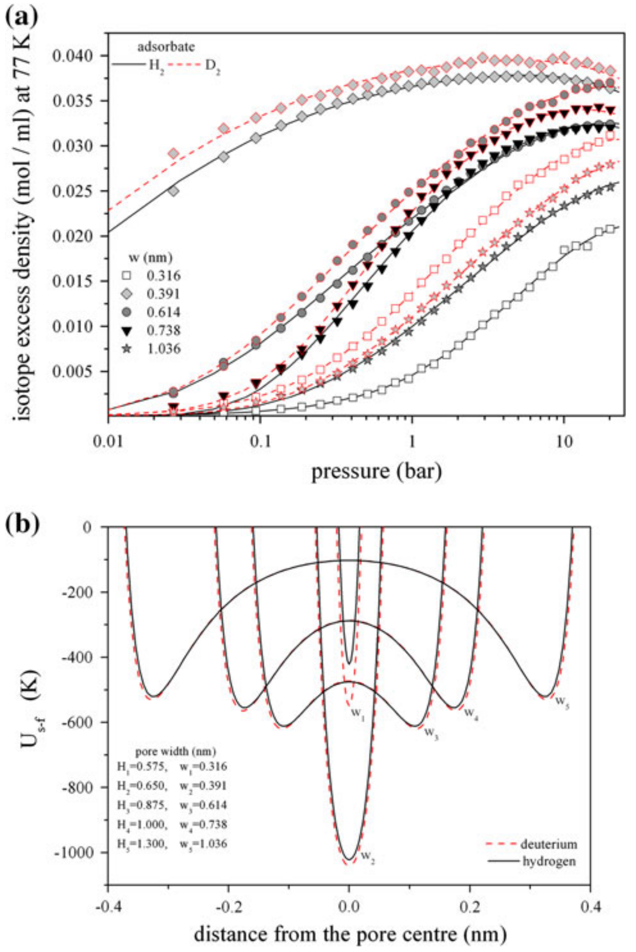

Fig. 1 **a** H_2 (*black symbols*) and D_2 (*red symbols*) excess adsorption densities at 77 K, for carbon slit pore models of 0.316 (*squares*), 0.391 (*diamonds*), 0.614 (*circles*), 0.738 (*triangles down*) and 1.036 (*stars*) nm chemical width. *Lines* can be used as a guide for the eye. **b** The impact of quantum effects on the solid–fluid interactions (Usf) for both adsorbates for different slit pore widths

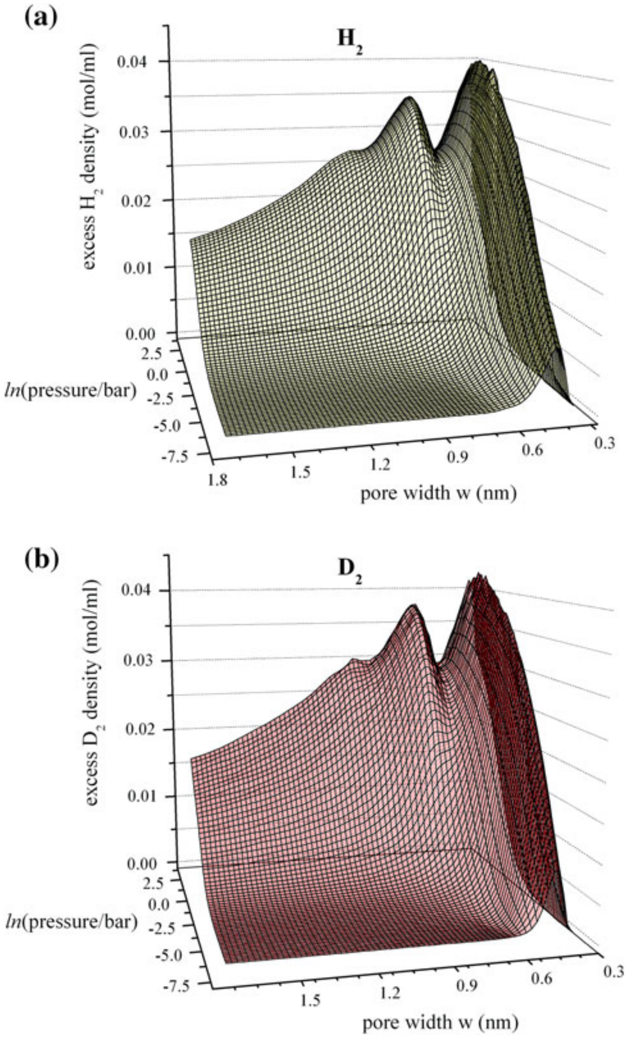

Fig. 2 $n(P, H)$ kernels of **a** H_2 and **b** D_2 adsorption in slit carbon pores at 77 K and up to pressures of 20 bar

molecular hydrogen, and as such the occurrence of quantum sieving effects is highly probable. This is confirmed by the respective considerably higher densities observed for deuterium compared to hydrogen. The 0.391 nm pore depicts the highest adsorption densities for both adsorbates in the low pressure range. This effective width induces optimal solid–fluid interactions as the potentials stemming from the two walls overlap at the pore center resulting to enhanced adsorption energy. Furthermore, the excess adsorption density in the specific pore obtains a negative slope at high pressures, for both H_2 and D_2. This is due to the fact that the pore has been already filled and the adsorbate cannot be further compressed inside the confined space. The 0.614 nm pore produces similar adsorption densities at zero coverage for both isotopes and quantum sieving (that practically initiates at around 0.1 bar) becomes more pronounced with pressure increase. In addition, this pore size can fairly accommodate two layers of adsorbate, in close contact with each wall of the slit. Due to the quantum effect the formation of deuterium layers is favored against the formation of hydrogen layers. Finally, the 0.738 nm and the 1.036 nm pores seem to be quite wide to have any considerable effect on the adsorption curves of the two isotopes which exhibit practically the same shape.

The collection of all model, single-pore adsorption isotherms, comprising the $n(P, H)$ kernels of Eq. 1, calculated for H_2 and D_2 are collectively shown in the three-dimensional grid of Fig. 2.

4.2 Calculated D_2/H_2 selectivity

The results from the single-component adsorption simulations were used for the calculation of the equilibrium selectivity of D_2 over H_2 at 77 K. The selectivity factor is expressed for simplicity as the ratio of the computed adsorption densities of the two gases within a given single pore over the respective density values in the bulk phase (bulk densities were computed by performing GCMC simulations in empty simulation volumes). Figure 3 illustrates the obtained selectivity matrix as a function of pressure and pore size. It can be seen that quantum sieving efficiency is limited as expected to the very fine pores where the effective width is comparable to hydrogen molecular size. The D_2/H_2 selectivity surface generally exhibits a decreasing slope towards a deep minimum at the pore size range 0.4–0.5 nm. A maximum of selectivity values is observed at around 0.6 nm, extending to the full pressure scale and becoming progressively pronounced with pressure. A second maximum appears at approximately 0.9 nm, implying that the increase of the effective pore width by one molecular diameter (i.e. 0.3 nm) can accommodate an additional layer of adsorbate within the confined pore space. Deuterium layers are formed faster as they are more localized due to stronger solid–fluid interactions, compared to hydrogen. However there is no further selectivity enhancement for pores larger than 1.2 nm pore, as in these cases quantum effects diminish. It should be noted, that such pore-size selectivity relations refer to model pore shapes (i.e. slits) with ideal carbon surfaces (homogeneous). In most cases, "real" materials differ from this simplified approach both structurally and energetically (narrow passages close to the outer surface and wider pores in-between, curved surfaces very rich in functional groups) (Koresh and Soffer 1980). On the other hand structural irregularities, may have a profound effect on the kinetic properties, nevertheless equilibrium characteristics stem from local confinement at the nanoscale, which is adequately captured by the slit pore model (this is why it is used to deduce pore size distributions of carbon materials).

4.3 Comparison with experimental data

For the characterization of Takeda 3A carbon it is impossible to use either N_2 or Ar as their sorption at low temperatures is severely hindered by kinetic and/or size exclusion reasons (in practice experimental isotherms reveal zero adsorption). On the contrary H_2 is supercritical at 77 K and its molecular diameter much smaller, so significant uptake is recorded. In this respect, in order to test the simulation approach described in the previous sections we have used the following strategy. Based on the experimental H_2 sorption isotherm and the GCMC simulated adsorption kernel for H_2 (described in Sect. 4.1) we deduced a pore size distribution for Takeda 3A. We then predicted a D_2 adsorption isotherm based on this pore size distribution and the GCMC D_2 kernels (Sect. 4.1). The latter can be directly compared with the experimental D_2 isotherm and conclusions on the quality of our approach can be drawn.

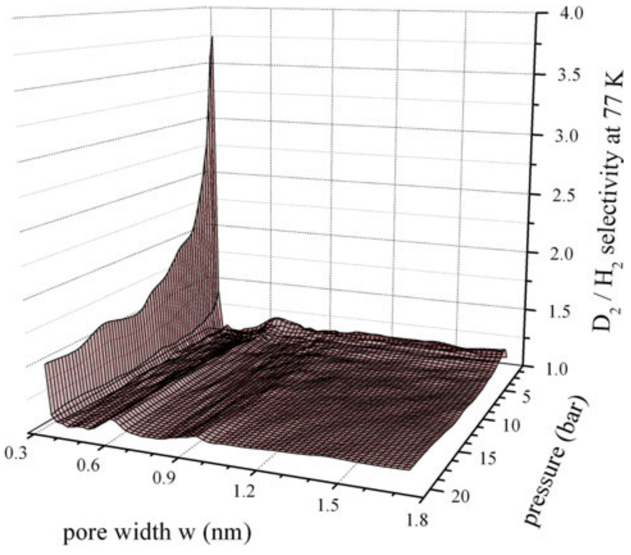

Fig. 3 D_2/H_2 equilibrium selectivity matrix

The approach is practically based on solving the adsorption integral of Eq. 1. For the case of hydrogen, $N(P)$ is the experimental isotherm, $n(P, H)$ is the H_2 GCMC kernel matrix and $f(H)$ is the pore size distribution sought. Likewise, for deuterium, $N(P)$ is the predicted isotherm, $n(P, H)$ is the D_2 GCMC kernel matrix and $f(H)$ the pore size distribution deduced from the H_2 adsorption data. Actually solving the adsorption integral in order to produce a pore size distribution is an ill-posed problem and for this reason we used the E04NCF least squares minimization routine of the NAG library to fit the kernel to the experimental data by posing a non-negative constraint to the resulting pore size distributions. The actual fitting results are presented in Fig. 4, while the hydrogen deduced volume distribution in Fig. 5. Given the simplicity of the employed approach, the deduced PSD seems to capture adequately the pore system of T3A revealing a significant pore volume in the ultramicropore region (<0.7 nm) with a peak around 0.4 nm and a secondary microporous system in the area of 1.2 nm, in good accordance with CO_2 derived PSDs but also in consistency with the properties of the material, which is actually a typical microporous sample that has been additionally treated in order to narrow the pores (or better the pore mouths) (Nguyen et al. 2009; Rutherford and Do 2000).

As explained before we used the pore size distribution of Fig. 5, the D_2 kernels and the adsorption integral in order to calculate a D_2 adsorption isotherm. This prediction is compared to the actual experimental data in Fig. 6. It is clearly seen that although not perfect, the predicted isotherm is in good agreement with our experimental data. At this point it

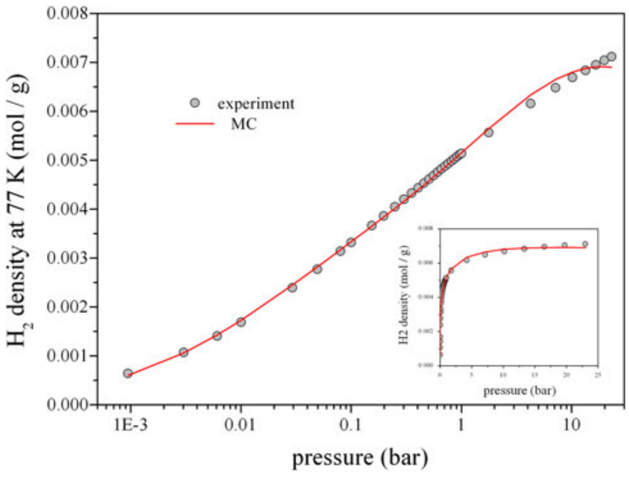

Fig. 4 Experimental (*points*) and fitted (*line*) H_2 adsorption isotherms at 77 K

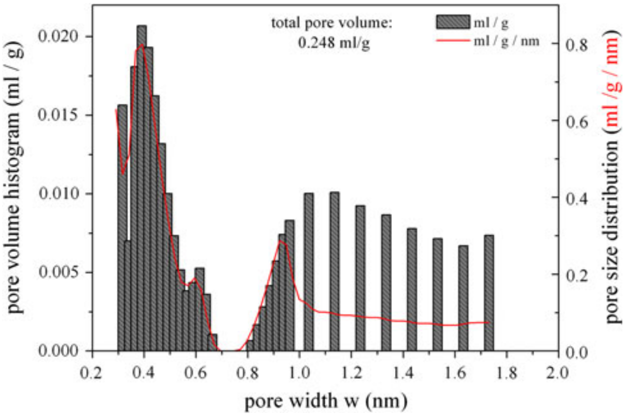

Fig. 5 H_2 deduced volume distribution (PSD) of T3A, based on experimental H_2 adsorption data and GCMC calculated H_2 adsorption isotherms. The volume histogram (ml/g) and the pore size distribution (ml/g/nm) refer to the first and the secondary axis, respectively

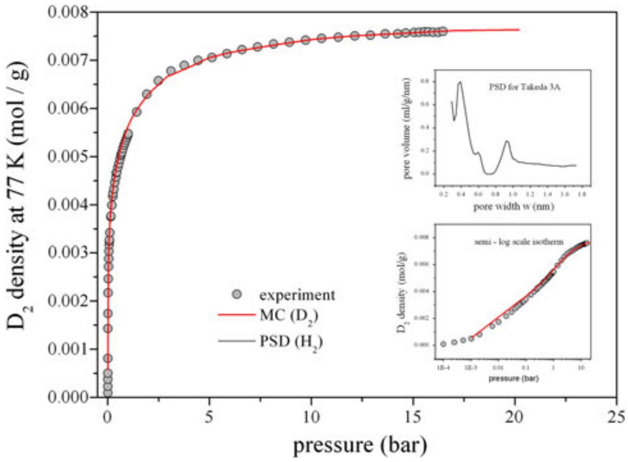

Fig. 6 Experimental (*points*) and predicted (*line*), D_2 adsorption isotherm at 77 K. The prediction is based on the T3A H_2 deduced PSD of Fig. 5 and the GCMC D_2 isotherms of Fig. 2b

should be stressed that our approach does not depend significantly on the choice of models either for the pore walls or for the fluid. More specifically we believe that similar results would have been produced if we had used mean-field graphitic walls or few-layers graphene walls instead of graphenes. The same holds for the H_2/D_2 models, where alternative interactions have been used in the literature. The reason is that both molecules have actually the same interactions with each other and the pore walls, but their differences are actually a quantum term that in algebraic terms is related with the derivatives of the LJ potentials.

5 Conclusions

High-pressure (up to 20 bar) H_2 and D_2 adsorption isotherms at 77 K were measured on the commercial carbon molecular sieve Takeda 3A with a nominal pore size in the range 0.3–0.4 nm. In parallel a GCMC approach, also including quantum corrections, was adapted for the simulation of H_2 and D_2 adsorption in single graphene slit-shaped pores with widths varying from 0.575 to 2.0 nm. The whole set of the model single-pore adsorption isotherms obtained for H_2 where used as kernel for the analysis of the experimental H_2 adsorption data towards the calculation of the Takeda 3A PSD. The deduced PSD captured adequately the pore system of T3A and enabled a good prediction of D_2 adsorption in the Takeda 3A carbon at 77 K and high pressures, as verified by the comparison with our experimental data, providing additional validation for our simulation approach.

Acknowledgments The authors wish to acknowledge partial support of the COST Action MP1103 “Nanostructured materials for solid–state hydrogen storage”.

References

Beenaker, J.J.M., Bordman, V.D., Krylov, SYu.: Molecular transport in subnanometer pores: zero-point energy, reduced dimensionality and quantum sieving. Chem. Phys. Lett. **232**, 379–382 (1995)

Cai, J., Xing, Y., Zhao, X.: Quantum sieving: feasibility and challenges for the separation of hydrogen isotopes in nanoporous materials. RSC Adv. **2**, 8579–8586 (2012)

Chen, B., Zhao, X., Putkham, A., Hong, K., Lobkovsky, E.B., Hurtado, E.J., Fletcher, A.J., Thomas, K.M.: Surface interactions and quantum kinetic molecular sieving for H_2 and D_2 adsorption on a mixed metal–organic framework material. JACS **130**, 6411–6423 (2008)

Do, D.D., Do, H.D.: Modeling of adsorption on nongraphitized carbon surface: GCMC simulation studies and comparison with experimental data. J. Phys. Chem. B. **110**, 17531–17538 (2006)

Dombrowski, R.J., Hyduke, D.R., Lastoskie, C.M.: Pore size analysis of activated carbons from argon and nitrogen porosimetry using density functional theory. Langmuir **16**, 5041–5050 (2000)

Garberoglio, G., Johnson, K.: Hydrogen isotope separation in carbon nanotubes: calculation of coupled rotational and translational states at high densities. ACS Nano **4**, 1703–1715 (2010)

Gauden, P.A., Terzyka, A.P., Kowalczyk, P.: Some remarks on the calculation of the pore size distribution function of activated carbons. J. Colloid Interface Sci. **300**, 453–474 (2006)

Gotzias, A., Steriotis, Th.: D_2/H_2 quantum sieving in microporous carbons: a theoretical study on the effects of pore size and pressure. Mol. Phys. **110**, 1179–1187 (2012)

Gregg, S.J., Sing, K.S.W.: Adsorption Surface Area and Porosity. Academic Press, New York (1982)

Hankel, M., Jiao, Y., Du, A., Gray, S.K., Smith, S.C.: Asymmetrically decorated, doped porous graphene as an effective membrane for hydrogen isotope separation. J. Phys. Chem. C **116**, 6672–6676 (2012)

Hattori, Y., Tanaka, H., Okino, F., Touhara, H., Nakahigashi, Y., Utsumi, S., Kanoh, H., Kaneko, K.: Quantum sieving effect of modified activated carbon fibers on H_2 and D_2 adsorption at 20 K. J. Phys. Chem. B. **110**, 9764–9767 (2006)

Inagaki, M.: New Carbons: Control of Structure & Functions, pp. 126–146. Elsevier, Amsterdam (2000)

Jagiello, J., Anson, A., Martınez, M.T.: DFT-based prediction of high-pressure H_2 adsorption on porous carbons at ambient temperatures from low-pressure adsorption data measured at 77 K. J. Phys. Chem. B. **110**, 4531–4535 (2006)

Jagiello, J., Thommes, M.: Comparison of DFT characterization methods based on N_2, Ar, CO_2, and H_2 adsorption applied to carbons with various pore size distributions. Carbon **42**, 1227–1232 (2004)

Kagita, H., Ohba, T., Fujimori, T., Tanaka, H., Hata, K., Taira, S., Kanoh, H., Minami, D., Hattori, Y., Itoh, T., Masu, H., Endo, M., Kaneko, K.: Quantum molecular sieving effects of H_2 and D_2 on bundled and nonbundled single-walled carbon nanotubes. J. Phys. Chem. C **116**(39), 20918–20922 (2012)

Kaneko, K., Itoh, T., Fujimori, T.: Collective interactions of molecules with an interfacial solid. Chem. Lett. **41**, 466–475 (2012)

Konstantakou, M., Steriotis, Th.A., Papadopoulos, G.K., Kainourgiakis, M., Kikkinides, E.S., Stubos, A.K.: Characterization of nanoporous carbons by combining CO_2 and H_2 sorption data with the Monte Carlo simulations. Appl. Surf. **253**, 5715–5720 (2007)

Koresh, J., Soffer, A.: Study of molecular sieve carbons. Part 1.-pore structure, gradual pore opening and mechanism of molecular sieving. J. Chem. Soc. Faraday I **76**, 2457–2471 (1980)

Kumar, A.V.A., Bhatia, S.K.: Quantum effect induced reverse kinetic molecular sieving in microporous materials. Phys. Rev. Lett. **95**, 24591–24595 (2005)

Kumar, A.V.A., Jobic, H., Bhatia, S.K.: Quantum effects on adsorption and diffusion of hydrogen and deuterium in microporous materials. J. Phys. Chem. B. **110**, 16666–16671 (2006)

Levesque, D., Gicquel, A., Darkrim, F.L., Kayiran, S.B.: Monte Carlo simulations of hydrogen storage in carbon nanotubes. J. Phys. Condens. Matter **14**, 9285–9293 (2002)

Liu, D., Wang, W., Mi, J., Zhong, C., Yang, Q., Wu, D.: Quantum sieving in metal-organic frameworks: a computational study. Ind. Eng. Chem. Res. **51**, 434–442 (2012)

Nguyen, T.X., Bhatia, S.K.: Characterization of accessible and inaccessible pores in microporous carbons by a combination of adsorption and small angle neutron scattering. Carbon **50**, 3045–3054 (2012)

Nguyen, T.X., Bae, J.-S., Wang, Y., Bhatia, S.K.: On the strength of the hydrogen–carbon interaction as deduced from physisorption. Langmuir **25**, 4314–4319 (2009)

Nguyen, T.X., Jobic, H., Bhatia, S.K.: Microscopic observation of kinetic molecular sieving of hydrogen isotopes in a nanoporous material. Phys. Rev. Lett. **105**, 085901 (2010)

Noguchi, D., Tanaka, H., Fujimori, T., Kagita, H., Hattori, Y., Honda, H., Urita, K., Utsumi, S., Wang, Z.-M., Ohba, T., Kanoh, H., Hata, K., Kaneko, K.: Selective D_2 adsorption enhanced by the quantum sieving effect on entangled single-wall carbon nanotubes. J. Phys. Condens. Matter **22**, 334207–334221 (2010)

Pantatosaki, E., Papadopoulos, G.K., Jobic, H., Theodorou, D.N.: Combined atomistic simulation and quasielastic neutron scattering study of the low-temperature dynamics of hydrogen and deuterium confined in NaX zeolite. J. Phys. Chem. B. **112**, 11708–11715 (2008)

Rodriguez-Reinoso, F., Linares-Solano, A.: Microporous systems of activated carbons as revealed by adsorption methods. In: Thrower, P.A. (ed.) Chemistry and Physics of Carbon, pp. 1–146. Marcel Dekker, New York (1988)

Rutherford, S.W., Do, D.D.: Characterization of carbon molecular sieve 3A. Langmuir **16**, 7245–7254 (2000)

Sese, L.M.: Feynman-Hibbs potentials and path integrals for quantum Lennard–Jones systems: theory and Monte Carlo simulations. Mol. Phys. **85**, 931–947 (1995)

Stan, G., Cole, M.W.: Hydrogen adsorption in nanotubes. J. Low Temp. Phys. **110**, 539–544 (1998)

Steele, W.A.: The physical interaction of gases with crystalline solids. Surf. Sci. **36**, 317–352 (1973)

Tanaka, H., Kanoh, H., Yudasaka, M., Iijima, S., Kaneko, K.: Quantum effects on hydrogen isotope adsorption on single-wall carbon nanohorns. JACS **127**, 7511–7516 (2005)

Tanaka, H., Noguchi, D., Yuzawa, A., Kodaira, T., Kanoh, H., Kaneko, K.: Quantum effects on hydrogen isotopes adsorption in nanopores. J. Low Temp. Phys. **157**, 352–373 (2009)

Viscor, D., Ferraro, A., Loiko, Yu., Mompart, J., Ahufinge, V.: Quantum-state storage and processing for polarization qubits in an inhomogeneously broadened Λ-type three-level medium. Phys. Rev. A **84**, 1–8 (2012)

Wang, Q., Challa, S.R., Sholl, D.S., Johnson, J.K.: Quantum sieving in carbon nanotubes and zeolites. Phys. Rev. Lett. **82**, 956–959 (1999)

Wang, Q., Johnson, J.K., Broughton, J.Q.: Path integral grand canonical Monte Carlo. J. Chem. Phys. **107**, 5108–5118 (1997)

Wang, Y., Bhatia, S.: Quantum effect-mediated hydrogen isotope mixture separation in slit pore nanoporous materials. J. Phys. Chem. C **113**, 14953–14962 (2009)

Xu, Q., Liu, D., Yang, Q., Zhong, C.: Molecular simulation study of the quantum effects of hydrogen adsorption in metal-organic frameworks: influences of pore size and temperature. Mol. Simul. **35**, 748–754 (2009)

Zhao, X., Villar-Rodil, S., Fletcher, A.J., Thomas, K.M.: Kinetic isotope effect for H_2 and D_2 quantum molecular sieving in adsorption/desorption on porous carbon materials. J. Phys. Chem. B. **110**, 9947–9955 (2006)